

Kinematic alpha effect in isotropic turbulence simulations

Sharanya Sur¹, Axel Brandenburg² and Kandaswamy Subramanian¹ *

¹*Inter-University Centre for Astronomy and Astrophysics, Post Bag 4, Ganeshkhind, Pune 411 007, India*

²*NORDITA, AlbaNova University Center, SE - 106 91 Stockholm, Sweden*

ABSTRACT

Using numerical simulations at moderate magnetic Reynolds numbers up to 220 it is shown that in the kinematic regime, isotropic helical turbulence leads to an alpha effect and a turbulent diffusivity whose values are independent of the magnetic Reynolds number, R_m , provided R_m exceeds unity. These turbulent coefficients are also consistent with expectations from the first order smoothing approximation. For small values of R_m , alpha and turbulent diffusivity are proportional to R_m . Over finite time intervals meaningful values of alpha and turbulent diffusivity can be obtained even when there is small-scale dynamo action that produces strong magnetic fluctuations. This suggests that small-scale dynamo-generated fields do not make a correlated contribution to the mean electromotive force.

Key words: magnetic fields — MHD — hydrodynamics – turbulence

1 INTRODUCTION

The generation and maintenance of large-scale magnetic fields in stars and galaxies is often studied within the framework of the mean-field dynamo (MFD); see, e.g., Moffatt (1978); Parker (1979); Krause & Rädler (1980). A particularly important driver of MFDs is the α -effect. For isotropic turbulence and weak magnetic fields, i.e. in the kinematic regime, the α -effect can be expressed purely in terms of the kinetic helicity. Research in recent years has mostly been concerned with clarifying the effects of nonlinearity, but there are serious uncertainties even in the linear (kinematic) regime. In particular, whether or not α can then be expressed in terms of the kinetic helicity depends on the applicability of the first order smoothing approximation (FOSA) or other closures used to calculate α . Such approaches become questionable when the magnetic Reynolds number, R_m , is large, i.e. when the magnetic diffusion time is long compared with the turnover time which, in turn, is comparable with the correlation time of the turbulence. In the high conductivity limit FOSA can only be applied if the correlation time for the velocity field is much smaller than the eddy turnover time. This is not the case for high Reynolds number turbulence, where the two time scales are equal, i.e. the Strouhal number is unity (Brandenburg & Subramanian 2005b, 2007), so FOSA should in principle break down. In this case all higher order terms need to be taken into account (Knobloch 1976). Furthermore, high R_m random flows typically lead to a fluctuation dynamo which leads to rapidly growing small-scale magnetic fields independent of the mean field. This also breaks the assumption made by FOSA that fluctuating fields are much smaller than the mean field.

The existence of α -effect and turbulent diffusion has been worrying dynamo researchers over several decades. Assuming

steady flow patterns, Childress (1979) found that motions that concentrate magnetic fields into thin flux sheets lead to an α -effect whose value diminishes with R_m like $R_m^{-1/2}$. But for an analogous helical motion which concentrates the field into an axial flux rope, α tends to a finite limit as $R_m \rightarrow \infty$. He conjectured that the latter estimate may be typical of steady three-dimensional motion. The validity of turbulent diffusion has been questioned by Piddington (1981). Calculations by Kraichnan (1976) suggest that α and turbulent diffusion converge to finite values for statistically isotropic velocity fields with gaussian statistics. However, numerical simulations (Drummond & Horgan 1986) using a frozen velocity field suggest that in the limit of large magnetic Reynolds numbers α tends to zero. Based on specific imposed (kinematic) flow patterns it has been suggested that there is no simple relation between α and helicity of the flow; see Courvoisier, Hughes & Tobias (2006). In fact, their results may suggest that in the kinematic regime, α exhibits a strong R_m dependence (for large R_m up to 2×10^5) and could change sign for $R_m \approx 20$ and long correlation times. It is important to emphasize that in the non-linear regime, i.e. for finite magnetic field strength and including the Lorentz force, a strong R_m dependence is now indeed well established (Cattaneo & Hughes 1996; Brandenburg 2001); see Brandenburg & Subramanian (2005a) for a review. However, in the following we shall be concerned with the purely linear regime.

In order to clarify the R_m dependence in the kinematic regime we perform numerical turbulence experiments where we adopt an externally imposed body force to drive the flow. This is a common technique applied in simulations and helps develop homogeneous and isotropic turbulence which is easier to handle analytically. While the calculation of α from a turbulence simulation is relatively straightforward by imposing a uniform magnetic field, the calculation of turbulent diffusion is more uncertain. One possibility is to determine the decay rate of an initial large-scale magnetic field (Yousef, Brandenburg & Rüdiger 2003). Another more

* E-mail: sur@iucaa.ernet.in (SS); brandenb@nordita.dk (AB); kandu@iucaa.ernet.in (KS)

reliable method is to calculate both α and turbulent diffusion tensors simultaneously by computing the mean electromotive force using a number of different nonuniform test fields in different directions and of different spatial structure (Schrinner et al. 2005, 2007). This is also the approach used in the present paper.

2 TEST-FIELD PROCEDURE

In MFD theory, one averages the induction equation to obtain the standard dynamo equation for the mean field $\overline{\mathbf{B}}$,

$$\frac{\partial \overline{\mathbf{B}}}{\partial t} = \nabla \times (\overline{\mathbf{U}} \times \overline{\mathbf{B}} + \overline{\mathcal{E}} - \eta \nabla \times \overline{\mathbf{B}}), \quad \nabla \cdot \overline{\mathbf{B}} = 0. \quad (1)$$

This averaged equation now has a new term, the mean electromotive force (emf) $\overline{\mathcal{E}} = \overline{\mathbf{u} \times \mathbf{b}}$, which crucially depends on the statistical properties of the small-scale velocity and magnetic fields, \mathbf{u} and \mathbf{b} , respectively. A central closure problem in MFD theories is to compute the mean emf $\overline{\mathcal{E}}$ and express it in terms of the mean field itself. Assuming that the mean field is spatially smooth, the mean emf $\overline{\mathcal{E}}$ can then be expressed in terms of the mean magnetic field and its first derivative in a manner

$$\overline{\mathcal{E}}_i = \alpha_{ij} \overline{B}_j + \eta_{ijk} \overline{B}_{j,k}, \quad (2)$$

where α_{ij} and η_{ijk} are turbulent transport coefficients written in tensorial form, and a comma denotes partial differentiation.

In numerical simulations, the full α_{ij} and η_{ijk} tensors are determined by first computing the mean emf using test fields in different directions and of different spatial structure (Schrinner et al. 2005, 2007). In what follows, we employ xy averages such that the resulting mean fields are expressible only as functions of z and t . Some details of the test field method applied to this case have already been described by Brandenburg (2005). Note that the solenoidality condition then gives, $\overline{B}_z = \text{const} = 0$. Hence, one only needs to compute the four components of α_{ij} and η_{ijk} with $i, j = 1, 2$. Here the numbers 1, 2, and 3 refer to Cartesian coordinate directions x, y, z . In order to obtain the $4 + 4 = 8$ unknown coefficients, we need the x and y components of 4 different test fields, \overline{B}_i^{pq} , where i, p , and q take values 1 and 2.

In order to compute the components α_{11} and η_{123} , for example, it suffices to consider the following two test fields,

$$\overline{\mathbf{B}}^{11} = \begin{pmatrix} \cos k_1 z \\ 0 \\ 0 \end{pmatrix}, \quad \overline{\mathbf{B}}^{21} = \begin{pmatrix} \sin k_1 z \\ 0 \\ 0 \end{pmatrix}. \quad (3)$$

Here k_1 is the smallest non-vanishing wavenumber in the domain, and $p = 1$ or $p = 2$ denotes whether we take a cosine or sine behaviour for the test field, and $q = 1$ or $q = 2$ depending on whether the non-zero component of \overline{B}_i^{pq} is the x -component or y -component respectively. We insert these test fields into the relation

$$\overline{\mathcal{E}}_i^{pq} = \alpha_{ij} \overline{B}_j^{pq} + \eta_{ij3} \overline{B}_{j,3}^{pq}. \quad (4)$$

Since $q = 1$, only the $j = 1$ (x -) component contributes to the sum over j above. For the two values of p and with index i unspecified, we have

$$\overline{\mathcal{E}}_i^{11} = \alpha_{i1} \cos k_1 z - \eta_{i13} k_1 \sin k_1 z, \quad (5)$$

$$\overline{\mathcal{E}}_i^{21} = \alpha_{i1} \sin k_1 z + \eta_{i13} k_1 \cos k_1 z. \quad (6)$$

Similarly, for test fields which only have non-zero y -components, that is with $q = 2$, one obtains a similar pair of equations with the same arrangement of cosine and sine functions, but with α_{i2} , η_{i23} in place of α_{i1} and η_{i13} . So, for each value of i one obtains

independent matrix equations for the unknown coefficients α_{ij} and η_{ij3} as

$$\begin{pmatrix} \alpha_{ij} \\ \eta_{ij3} k_1 \end{pmatrix} = \mathbf{M}^{-1} \begin{pmatrix} \overline{\mathcal{E}}_i^{1j} \\ \overline{\mathcal{E}}_i^{2j} \end{pmatrix}, \quad (7)$$

where

$$\mathbf{M} = \begin{pmatrix} \cos k_1 z & -\sin k_1 z \\ \sin k_1 z & \cos k_1 z \end{pmatrix} \quad (8)$$

is the same matrix for each value of q and each of the two components $i = 1, 2$ of $\overline{\mathcal{E}}_i^{pq}$. Note that $\det \mathbf{M} = 1$, so the inversion procedure is well behaved and trivial.

Given the form of the test fields, we can compute the mean electromotive force $\overline{\mathcal{E}}^{pq} = \overline{\mathbf{u} \times \mathbf{b}^{pq}}$ for a given test field $\overline{\mathbf{B}}^{pq}$. The mean emf $\overline{\mathcal{E}}^{pq}$ is computed by solving the equations

$$\frac{\partial \mathbf{b}^{pq}}{\partial t} = \nabla \times (\overline{\mathbf{U}} \times \mathbf{b}^{pq} + \mathbf{u} \times \overline{\mathbf{B}}^{pq}) + \mathbf{G}^{pq} + \eta \nabla^2 \mathbf{b}^{pq} \quad (9)$$

for each test field $\overline{\mathbf{B}}^{pq}$ along with the momentum equation for the fluctuating velocity field (see further below).¹ Here

$$\mathbf{G}^{pq} = \nabla \times (\mathbf{u} \times \mathbf{b}^{pq} - \overline{\mathbf{u} \times \mathbf{b}^{pq}}) \quad (10)$$

is a nonlinear term that would normally be neglected under FOSA, but will be retained in the numerical simulations. For sufficiently large values of R_m the small-scale field \mathbf{b}^{pq} can grow exponentially due to small-scale dynamo action. An important question to ask is whether the predictions of FOSA work even in the presence of such a small-scale dynamo.

We adopt an isothermal equation of state with constant speed of sound, c_s , so the momentum and continuity equations are

$$\frac{\partial \mathbf{u}}{\partial t} = -\mathbf{u} \cdot \nabla \mathbf{u} - c_s^2 \nabla \ln \rho + \mathbf{f} + \rho^{-1} \nabla \cdot 2\rho \nu \mathbf{S}, \quad (11)$$

$$\frac{\partial \ln \rho}{\partial t} = -\mathbf{u} \cdot \nabla \ln \rho - \nabla \cdot \mathbf{u}, \quad (12)$$

where \mathbf{f} is a random forcing function consisting of circularly polarized plane waves with positive helicity and random direction, \mathbf{S} is the traceless rate of strain tensor. The length of the wavevector of the forcing function, $|\mathbf{k}_f|$, is chosen to be between 4.5 and 5.5, so the average is around $k_f = |\mathbf{k}_f| \approx 5$. The ratio k_f/k_1 is referred to as the scale separation ratio. It must be large enough to ensure that higher derivatives in equation (2) can be ignored and that a large-scale field could grow, if it was allowed to do so. For fully helical turbulence, a ratio of 5 is already sufficient, but 2.3 is not; see Fig. 23 of Haugen, Brandenburg, & Dobler (2004). We adjust the strength of the forcing such that the flow remains clearly subsonic (mean Mach number is below 0.2), so for all practical purposes the flow can be considered nearly incompressible. The details of the forcing function used in the present work can be found in Appendix A of (Brandenburg & Subramanian 2005b).

We do not include the Lorentz force in the momentum equation since we want to study the mean emf in the purely kinematic limit. We ignore here the possibility of a mean flow; such flows have not been seen to emerge under the simple conditions considered here. In the following we use the PENCIL CODE², where the test field algorithm has already been implemented. We employ periodic boundary conditions and use a resolution of up to 512^3

¹ Note that in the corresponding expression (27) of Brandenburg (2005) the $\overline{\mathbf{U}}$ term is incorrect. This did not affect his results because $\overline{\mathbf{U}} = 0$.

² <http://www.nordita.org/software/pencil-code>

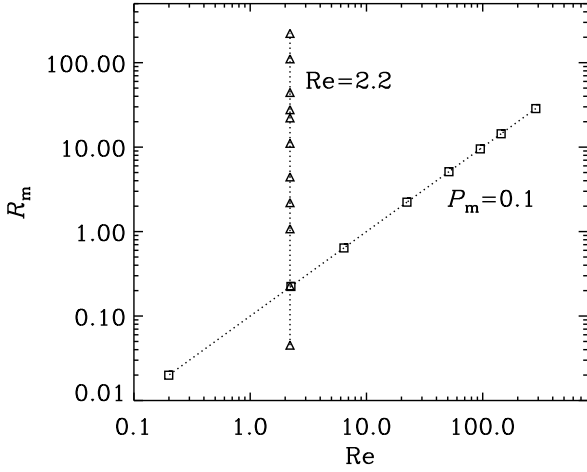


Figure 1. Parameters space covered by the simulations presented in this paper.

meshpoints for the run with the largest fluid Reynolds number. We use a domain of size $(2\pi)^3$, so the smallest wavenumber is $k_1 = 1$.

3 RESULTS

We are particularly interested in the dependence of α_{ij} and η_{ij3} on R_m and have considered cases where either the fluid Reynolds number was fixed, $Re = u_{rms}/(\nu k_f) = 2.2$, or where $Re = 10R_m$, corresponding to a magnetic Prandtl number of $P_m = \nu/\eta = 0.1$; see Fig. 1.

The flow is isotropic and, not surprisingly, we find that, to a good approximation, the α and η_t tensors are isotropic with

$$\alpha_{11} = \alpha_{22} \equiv \alpha, \quad \eta_{123} = -\eta_{213} \equiv \eta_t, \quad (13)$$

and $\alpha_{12} = \alpha_{21} = \eta_{113} = \eta_{223} = 0$. The quantity η_t is simply referred to as turbulent magnetic diffusivity. Although the code is capable of solving for the full α_{ij} and η_{ij3} tensors, we simplify matters by solving only for α_{i1} and η_{i13} using just two test fields.

We present the results for α and η_t normalized to the respective expressions obtained using FOSA for large magnetic Reynolds numbers (Moffatt 1978; Krause & Rädler 1980),

$$\alpha_0 = -\frac{1}{3}\tau\overline{\boldsymbol{\omega} \cdot \mathbf{u}}, \quad \eta_{t0} = \frac{1}{3}\tau\overline{\mathbf{u}^2}, \quad (14)$$

where τ denotes the correlation time of the turbulence. Using the definitions of the Strouhal number,

$$St = \tau u_{rms} k_f \quad (15)$$

and the fact that $St \approx 1$ for large enough magnetic Reynolds numbers (Brandenburg & Subramanian 2005b, 2007), we expect

$$\alpha_0 = -\frac{1}{3}u_{rms}, \quad \eta_{t0} = \frac{1}{3}u_{rms}k_f^{-1} \quad (16)$$

for a flow that is maximally helical and has positive helicity. For $R_m < 1$ the relevant value of τ is no longer the dynamical time scale, $(u_{rms}k_f)^{-1}$, but the resistive one, $(\eta_t k_f^2)^{-1}$. Therefore, both α/α_0 and η_t/η_{t0} have to be scaled by R_m for $R_m < 1$.

The test field procedure yields α and η_t as functions of z and t . Since the turbulence is homogeneous, we average these data first over z and calculate then time averages over the full time series.

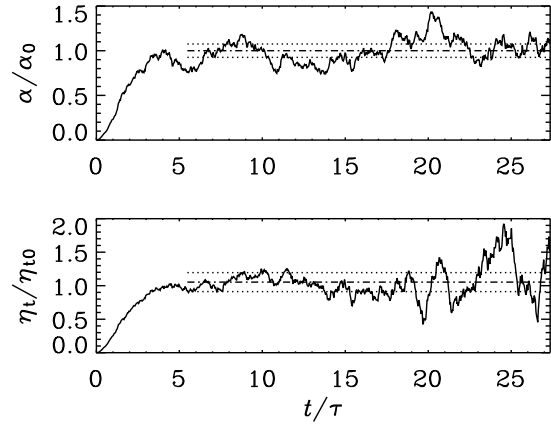


Figure 2. Time series of the z averaged values α and η_t for $R_m = 220$ and $Re = 2.2$. Time is expressed in turnover times, $\tau = (u_{rms}k_f)^{-1}$. Dash-dotted lines give the time average and dotted lines mark error margins obtained by averaging over subsections of the full time series (see text). In this run there is small-scale dynamo action leading to strong fluctuations for $t/\tau > 25$, making the determinations of reliable averages harder at late times.

An example of such a time series is shown in Fig. 2 for $Re = 2.2$ and $R_m = 220$. Note that even for $R_m \gg 1$ the time averages of α/α_0 and η_t/η_{t0} are close to unity, i.e. the predictions from FOSA appear to be reasonably accurate. We use such time series to calculate error bars as the maximum departure between these averages and the averages obtained from one of three equally long subsections of the full time series.

The degree of fluctuations in the time series of α and η_t is quite moderate and not at all as strong as in the nonlinear regime where fluctuations of α can even dominate over the mean value (Cattaneo & Hughes 1996). The latter is likely to be a consequence of a very small (catastrophically quenched) mean value in the nonlinear regime. On the other hand, in the kinematic regime the level of fluctuations is found not to vary significantly with R_m ; see Fig. 3. A weak R_m dependence has also been found in the presence of shear (Brandenburg et al. 2007), where such fluctuations can contribute to dynamo action by an incoherent α effect (Vishniac & Brandenburg 1997). However, at late times, i.e. toward the end of the simulation, the degree of fluctuations increases (Fig. 2). This has to do with the emergence of small-scale dynamo action that leads to the production of strong small-scale magnetic fields, \mathbf{b}^{pq} , although this does not affect the resulting time averaged emf for a reasonably long stretch of time.

In our simulations with $Re = 2.2$, small-scale dynamo action with exponential growth of the rms value of \mathbf{b}^{pq} is found when R_m is larger than a certain critical value $R_{m,cr}$ that seems to be somewhere between 28 and 44; see Fig. 4 which shows the growth of the rms value of \mathbf{b}^{pq} for $R_m = 220$ and $P_m = R_m/Re = 100$.

On the other hand, for $R_m < R_{m,cr}$ the rms value of the small-scale field settles to a constant value. In the supercritical case the magnetic field is highly intermittent in the sense that only in a few places the magnetic field reaches large positive and negative values; see Fig. 5. Such intermittency is typical of large- P_m small-scale dynamo action in the kinematic stage (Zeldovich, Ruzmaikin & Sokoloff 1990; Brandenburg & Subramanian 2005a).

The corresponding normalized values of α and η_t as a function of R_m are shown in Fig. 6, for the case when $Re = 2.2$. Fig. 7

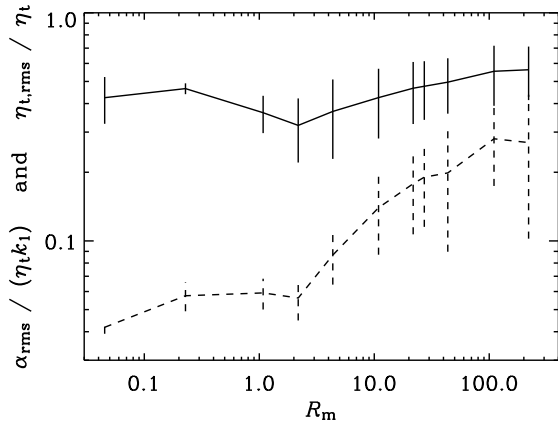


Figure 3. Dependences of α_{rms} (normalized by $\eta_{t0}k_1$, solid line), and $\eta_{t,\text{rms}}$ (normalized by η_{t0} , dashed line), on the magnetic Reynolds number for $\text{Re} = 2.2$. The vertical bars denote the error estimated by averaging over subsections of the full time series.

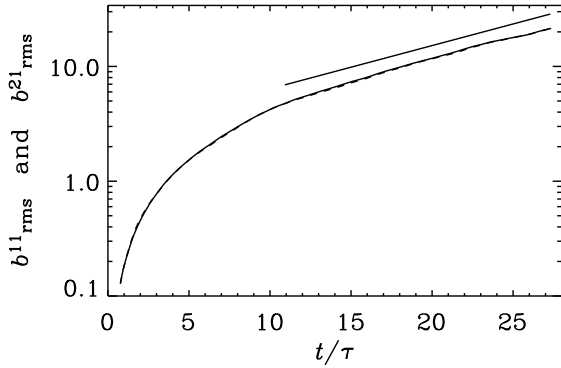


Figure 4. Evolution of the root-mean-squared value of the small-scale magnetic fields b^{11} for $\text{Re} = 2.2$ and $R_m = 220$. (The result for b^{21} is overplotted as a dashed line, but it is almost indistinguishable from the solid line for b^{11} .) Note the nearly exponential growth for $t/\tau > 10$, as illustrated by the straight line with a slope corresponding to a growth rate of $1.55\tau^{-1}$.

shows the results for simulations with $P_m = 0.1$. It turns out that in all cases with $R_m > 1$, $\alpha/\alpha_0 \approx \eta_t/\eta_{t0} \approx 1$, while for $R_m < 1$ these ratios are equal to R_m .

Also in the case with $P_m = 0.1$, where we explore larger values of Re up to 300, α/α_0 and η_t/η_{t0} reach values close to unity.

We may conclude that for isotropic homogeneous turbulence the high conductivity results obtained under FOSA are reasonably accurate up to the moderate values of R_m that we have tested. Interestingly, this conclusion is obtained even in the presence of a small-scale dynamo, where b is growing exponentially. Conversely, when different values of α and η_t are found under specific circumstances, then this must be related to the nature of these circumstances and does not indicate the break down of FOSA in general.

How is it then possible that the high conductivity limit of FOSA works even though the correlation time of the velocity field is comparable to the eddy turnover time? A possible reason for this could be that in the kinematic regime the high conductivity limit of FOSA gives similar predictions than the minimal τ approxima-

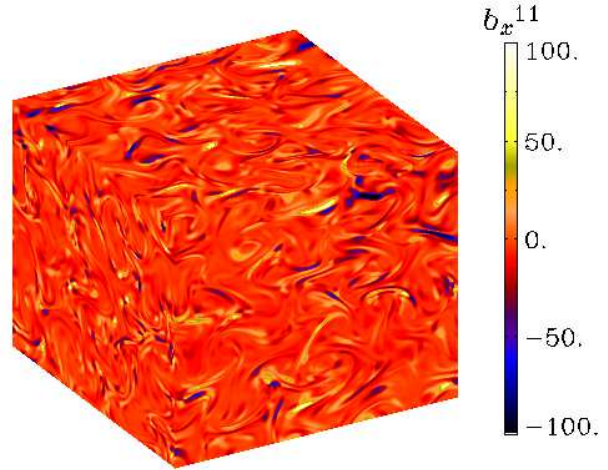


Figure 5. Colour-coded (or grey-scale) representation of b_x^{11} on the periphery of the box for a run with $\text{Re} = 2.2$ and $R_m = 220$ at $t/\tau = 28$. The colour/grey scale has been clipped at ± 100 , even though the extrema are at ± 200 . Note the extreme intermittency as evidenced by the presence of extended nearly field-free regions.

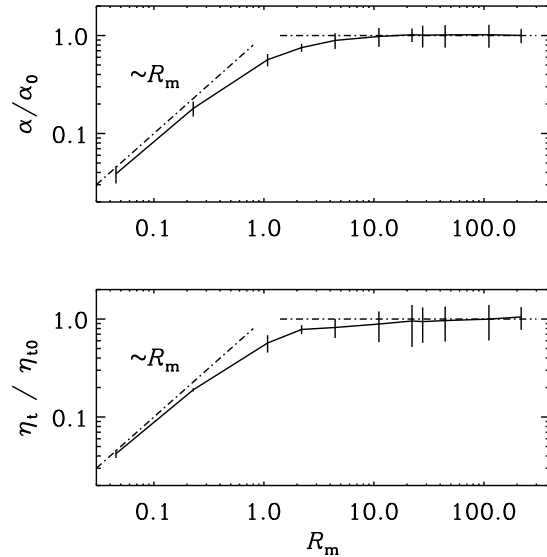


Figure 6. Dependence of the normalized values of α and η_t on R_m for $\text{Re} = 2.2$. The vertical bars denote twice the error estimated by averaging over subsections of the full time series (see text). The run with $R_m = 220$ ($\text{Re} = 2.2$) was done at a resolution of 512^3 meshpoints.

tion (MTA) where the triple correlations are not neglected, but replaced by the quadratic correlations divided by a turnover time. This closure assumption is not well justified, although numerical simulations (for $R_m \leq 300$) support some aspects of this closure (Brandenburg & Subramanian 2005b, 2007). Let us also emphasize that in this work we have not probed two particular aspects where FOSA and MTA depart from each other: feedback from helical mean fields (see Brandenburg & Subramanian 2005a, for a review), and strong time dependence. In the latter case a time

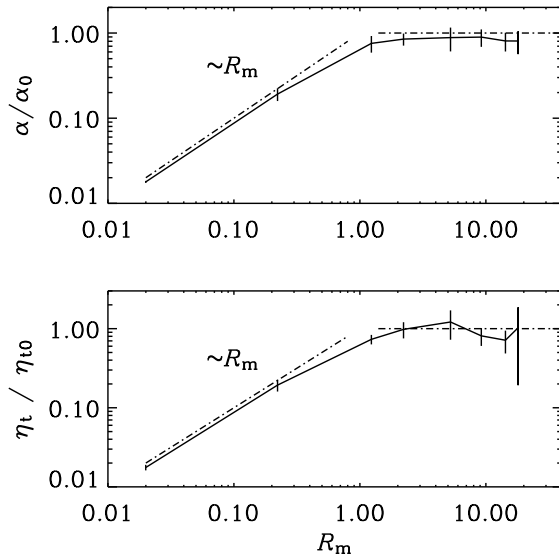


Figure 7. Same as Fig. 6, but for $P_m = 0.1$. The run with $R_m \approx 22$ ($Re \approx 220$) required a resolution of 512^3 meshpoints.

derivative of $\bar{\mathcal{E}}$ would be important in giving the mean field equation the character of a wave equation (Blackman & Field 2002; Brandenburg, Käpylä, & Mohammed 2004).

4 CONCLUSIONS

The present work has shown that for isotropic turbulence the first order smoothing results give quite accurate expressions for the α effect and the turbulent magnetic diffusivity in the kinematic regime. This result comes almost as a surprise given that in recent years mean field theory has been seriously challenged based on numerical simulations. However, we can now clearly say that for moderate Reynolds numbers up to about 220 and under the conditions stated (scale separation, isotropy, etc.) there is *no* evidence that the kinematic results obtained using FOSA are flawed, even though its applicability can then no longer be guaranteed and we know of its shortcomings in the nonlinear regime (Brandenburg & Subramanian 2005a). As explained above, a possible reason for this might be that the predictions of FOSA and MTA are rather similar, even though FOSA loses its justification whilst MTA hinges on a not well justified closure hypothesis.

The emergence of small-scale dynamo action for supercritical values of R_m of about 30 does not seem to affect the average values of α and η_t . This suggests that the exponentially growing part of the small-scale field does not make a contribution to the mean emf $\bar{\mathcal{E}}$, correlated with the imposed test fields. However, small-scale dynamo action makes the calculation of reliable average values of α and η_t more difficult. Of course, in the supercritical case the long time limit of any kinematic problem becomes unphysical. Nevertheless, within a certain time interval the averaged values of α and η_t match reasonably with theoretical expectations of FOSA.

ACKNOWLEDGMENTS

SS and KS thank Nordita for hospitality during the course of this work. SS would like to thank the Council of Scientific and Indus-

trial Research, India for providing financial support. We acknowledge the use of the HPC facility (Cetus cluster) at IUCAA.

REFERENCES

- Blackman E. G., Field G. B. 2002, Phys. Rev. Lett., 89, 265007
 Brandenburg A. 2001, ApJ, 550, 824
 Brandenburg A. 2005, AN, 326, 787
 Brandenburg A., Subramanian K. 2005a, Phys. Rep., 417, 1
 Brandenburg A., Subramanian K. 2005b, A&A, 439, 835
 Brandenburg A., Subramanian K. 2007, AN, 328, 507
 Brandenburg, A., Käpylä, P., & Mohammed, A. 2004, Phys. Fluids, 16, 1020
 Brandenburg, A., Rädler, K.-H., Rheinhardt, M., & Käpylä, P. J. 2007, ApJ, (submitted) arXiv 0710.4059
 Cattaneo F., Hughes D. W. 1996, Phys. Rev. E, 54, R4532
 Childress S. 1979, Phys. Earth Planet. Int. 20, 172.
 Courvoisier A., Hughes D. W., Tobias S. M. 2006, Phys. Rev. Lett., 96, 034503
 Drummond I. T., Horgan R. R. 1986, J. Fluid Mech., 163, 425
 Haugen N. E. L., Brandenburg A., Dobler W. 2004, Phys. Rev. E, 70, 016308
 Knobloch E. 1978, ApJ, 225, 1050
 Kraichnan R. H. 1976, J. Fluid Mech., 75, 657
 Kraichnan R. H. 1979, Phys. Rev. Lett., 42, 1677
 Krause F., Rädler K.-H. 1980, Mean-field magnetohydrodynamics and dynamo theory (Pergamon Press, Oxford)
 Moffatt H. K. 1978, Magnetic field generation in electrically conducting fluids (Cambridge University Press, Cambridge)
 Parker E. N. 1979, Cosmic magnetic fields (Clarendon Press, Oxford)
 Piddington J. H. 1981, ApJ, 247, 293
 Schrunner M., Rädler K.-H., Schmitt D., Rheinhardt M., Christensen U. 2005, AN, 326, 245
 Schrunner M., Rädler K.-H., Schmitt D., Rheinhardt M., Christensen U. 2007, Geophys. Astrophys. Fluid Dyn., 101, 81
 Vishniac, E. T., & Brandenburg, A. 1997, ApJ, 475, 263
 Yousef T. A., Brandenburg A., & Rüdiger G. 2003, A&A, 411, 321
 Zeldovich, Y. B., Ruzmaikin, A. A. & Sokoloff, D. D. 1990, The almighty chance (World Scientific, Singapore)